Science of Sintering, **52** (2020) 163-176

doi:https://doi.org/10.2298/SOS2002163S

UDK: 676.017.5; 553.689; 621.926.087; 665.7.035.8

Evolution of Structural and Functional Properties of the $Fe/BaTiO_3$ System Guided by Mechanochemical and Thermal Treatment

Nemanja Stojanović[1], Aleksandra Kalezić-Glišović[1*)], Aco Janićijević[2], Aleksa Maričić[1]

[1]Joint Laboratory for Advanced Materials of SASA, Section for Amorphous Materials, Faculty of Technical Sciences Čačak, University of Kragujevac, 32102 Čačak, Serbia

[2]Faculty of Technology and Metallurgy, University of Belgrade, 11120 Belgrade, Serbia

Abstract:

Multiferroic systems are attractive to the researches worldwide due to diversity of existing applications, as well as possible novel ones. In order to contribute to understanding of the processes that take place within the structure of such a system, we subjected it to mechanochemical activation and thermal treatment. Powdery mixtures of iron and barium titanate in a mass ratio of 30% Fe and 70% $BaTiO_3$ were activated in a planetary ball mill for time duration of 30 to 300 min and subsequently sintered at 1200 °C in the atmosphere of air. During the activation the system undergoes structural phase transitions, whereby the content of iron and its oxides changes. The highest Fe content was observed in the sample activated for 270 min, with local maxima in crystallite size and microstrain values and a minimum in dislocation density. The complex dielectric permittivity changes in the applied radio frequency field, rangingfrom 176.9 pF/m in thesample activated for 90 min to 918.1 pF/m in the sample activated for 180 min. As the frequency of the field increases, an exponential decrease in the magnetic with a simultaneous increase in the electrical energy losses is noticeable. The system exhibits ferromagnetic resonance, whereby longer activation in the mill shifts the resonant frequency to higher values. Negative electrical resistance was observed in all analyzed samples. The activation time changes both the demagnetization temperature and the Curie temperature of the samples undergoing heating and cooling cycles in the external permanent magnetic field. Curie temperature is the highest in the sample activated for 240 min. Thermal treatment increases the initial magnetization of all samples, with the most pronounced increase of ~95% in the sample activated for 300 min.

Keywords*: Barium titanate; Milling; Structure; Electrical properties; Magnetic properties.*

1. Introduction

The existence of multiferroic materials and possible magnetoelectric coupling in solid systems was first predicted by Curie in 1894, based on the consideration of symmetry in crystals [1, 2].Fundamental research in solid state physics, aided by the great advances in experimental technique achieved in the mid-twentieth century, has led to the full affirmation

*) **Corresponding author:**aleksandra.kalezic@ftn.kg.ac.rs

of materials science, which is in the last decade experiencing its second renaissance. Multiferroic materials are in the focus of extensive scientific research by virtue of their coexisting ferroelectric and ferromagnetic properties which could possibly be manipulated at room temperature, allowing the use of these materials in various promising technologies, from highly sensitive detection of weak magnetic fields to quantum electromagnetics and magnetoelectric data storage [3-6].The latter is of great importance, given the enormous and ever-increasing amount of digital data that emerges every day (quintillion of bytes in 2019 only) which is most commonly stored in magnetized media in the form of oppositely polarized magnetic domains.Due to the magnetoelectric effect, i.e. inducing magnetization by an electric field or causing polarization by a magnetic field, multiferroics could be utilized to store magnetic data governed by the applied electric field [7].The search for realization and practical use of such properties contained within a single phase, dating back to the pioneering research of the magnetoelectric effect in multiferroic materials in 1950s [8], continues with new discoveries and synthesis of various multiferroic systems whose structural and, consequently, functional properties could be a priori tailored.

Barium titanate (BTO) is a well-studied perovskite structure ferroelectric belonging to a class of materials known as “frustrated magnets” [9], in which the appearance of both ferroelectricity and magnetism is closely related to the structural distortion of the crystal lattice [10].The flexibility of the BTO structure allows for the accommodation of a large number of various dopants, including iron. Transition metal doping is a good way to induce magnetism in otherwise non-magnetic barium titanate, with the incorporation of dopants into the BTO lattice largely determined by the ionic radii of the participants in the process [11]. Albeit comprehensively investigated over the years, BTO-based ceramics persist to inspire novel research approaches [12, 13] remaining at the forefront of materials science.

In an effort to contribute to the understanding of properties of the multiferroic Fe/$BaTiO_3$ system (BFTO) of a particular composition, the influence of the mechanochemical activation time and heating temperature of activated BFTO powders on its functional properties, as well as on the accompanying evolution of different crystalline phases, was in this study examined.

2. Materials and Experimental Procedures

Fine powders of pure iron (Aldrich, St. Louis, MO, 99.99%) and barium titanate (Aldrich, St. Louis, MO, 99%) were mixed mechanically into the initial mixture with a ratio of 30 mass% Fe and 70 mass% $BaTiO_3$. This initial powder was activated in a planetary mill with zirconium oxide balls (Retsch PM 400) for time duration of 30 min, 60 min, 90 min, 120 min, 150 min, 180 min, 210 min, 240 min, 270 min and 300 min in the air atmosphere with a rotational speed of 400 rpm. After the milling samples were pressed into tablets (discs) and toroids under pressure of 392 MPa and 1 GPa successively and then sintered [14] in the air atmosphere of a laboratory oven for 2 h at 1200 °C. Investigation of the sintered samples surface was performed using Carl Zeiss Jena optical microscope, with a 50W halogen lamp and a 100x magnification.

Crystalline phases of the activated powders were determined using a Bruker D8 diffractometer with Bragg-Brentano geometry, using filtered $CuK\alpha_1$ and $CuK\alpha_2$ radiation lines with wavelengths of 0.15405929 nm and 0.15444274 nm, in the 2θ recording range from 10° to 120° and with a recording step of 0.01°. Change in the content of iron and its oxides in the system with increasing activation time was monitored by comparing their relative intensities. The average crystallite sizes (D_{hkl}) and microstrain values (ε_{hkl}) were estimated by the Williamson-Hall method [15] based on a graphical interpretation of the Debye-Scherrer relation [16], while dislocation densities (ρ_D) were determined using the well-known Williamson-Smallman equation [17], assuming the isotropy of dislocations in the material.

Electrical and magnetic measurements of the samples were performed on a HP 4191A multifrequency LCR instrument, in the frequency range from 0 MHz to 500 MHz. Changes in the value of complex dielectric constant were monitored for the samples activated for 90-300 min and the energy losses in the system were estimated by calculating the electrical dissipation factor and magnetic losses. Complex magnetic permeability and electrical resistance were determined for toroidal samples activated for 120 min, 180 min and 240 min, with different number of coils (11 coils for the sample activated for 120 min and 10 coils for samples activated for 180 min and 240 min).

For samples activated for 90 min, 120 min, 240 min and 300 min, changes in the mass magnetization value were observed in two successive heating and cooling cycles in the temperature range from 20 °C to 600 °C. These measurements were performed according to a modified Faraday method [18] using a laboratory weighing scale (Sartorius PRACTUM 124-1S) with a sensitivity of 10^{-7} kg and a magnetic field strength at the sample placement site of 50 kA/m. For these samples, the temperature values of characteristic phase transitions – partial demagnetization temperature and Curie temperature were determined.

3. Results and Discussion

Microscopy of the sintered samples showed a difference in the granulation and color of the surface of samples activated for 30 min, 60 min and 90 min compared to the others. White spots that may originate from the titanate were observed. The tablets were pale gray and crumbled upon handling, indicating poor homogenization of the initial Fe and BTO powders for the given milling times. Samples activated for 120-300 min were more homogenized and mechanically more stable. The same dark gray color of the surface leads to the conclusion that the milling time in these samples does not significantly affect merging of the initial powders.

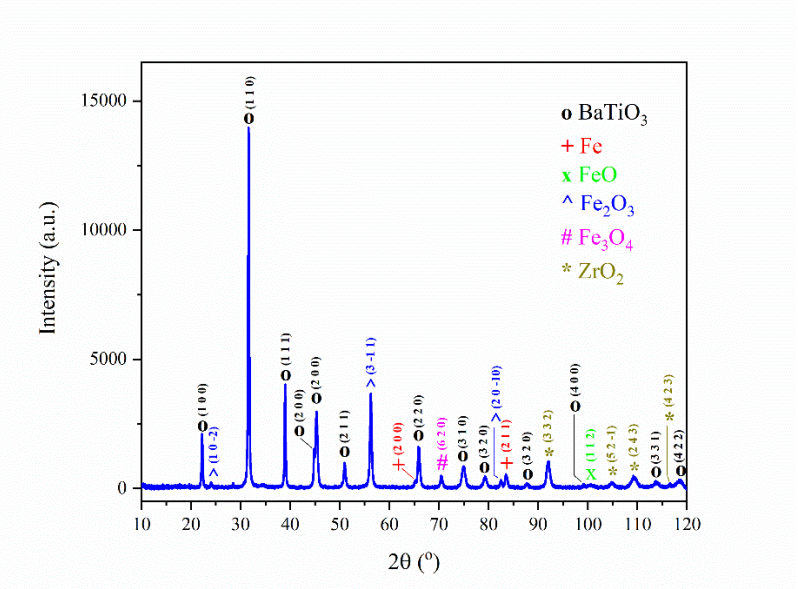

Fig. 1. XRD pattern of the Fe/$BaTiO_3$ powder sample activated for 30 min, with identified phases and Miller indices of Bragg reflection planes.

During activation, iron reacts with oxygen from the air transitioning to its oxide forms – FeO, Fe_2O_3 and Fe_3O_4 – who's content in the initial powder changes depending on the time of activation. X-ray diffraction (XRD) pattern of the sample activated for 30 min (Fig. 1) exhibits results of the peak assignment. Bragg reflection planes were indexed by using and

comparative analysis of the resources of two independent crystallographic databases: the Crystallography Open Database (COD) [19, 20] and the Materials Project (MP) [21, 22]. Completeness and consistency of XRD patterns contained in these bases with the experimental ones were verified by comparison with XRD patterns simulated in VESTA [23], with predefined experimental conditions. The presence of zirconium dioxide in the samples originates most likely from the milling balls in a planetary mill. Fig. 2 shows XRD patterns of the samples for all activation times. It is noticeable that the intensity of (110) reflection of barium titanate decreases, whilst the intensity of (200) reflection rises. With the increase of milling time leading to introduction of Fe into the BTO structure, barium titanate changes its crystallinity by moving from local orthorhombic and tetragonal to predominantly cubic symmetry due to the influence of size of crystalline grains [24].

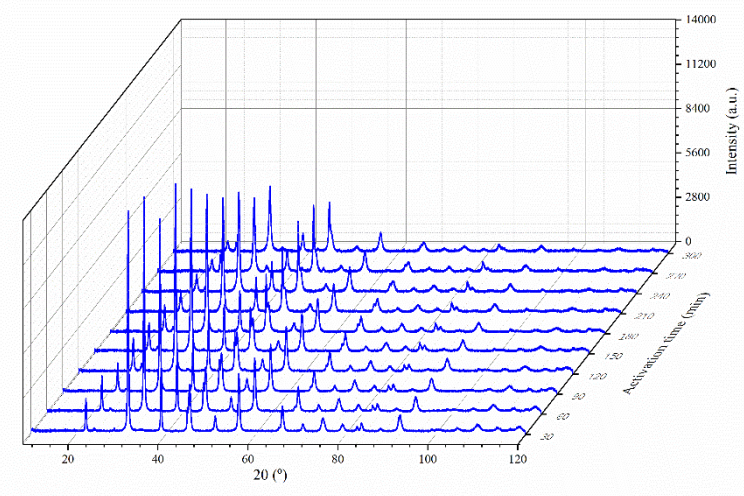

Fig. 2. XRD patterns of the Fe/$BaTiO_3$ system for various activation times ranging from 30 min to 300 min.

Tab. I Values of microstructure parameters of the Fe/$BaTiO_3$ system for various activation times.

Activation time (min)	D_{hkl} (nm)	ε_{hkl} (%)	ρ_D (nm^{-2})
30	110 ± 1	0.11 ± 0.01	249 ± 1
60	137 ± 1	0.13 ± 0.01	161 ± 1
90	112 ± 1	0.13 ± 0.01	238 ± 1
120	72 ± 1	0.11 ± 0.01	572 ± 1
150	64 ± 1	0.12 ± 0.01	744 ± 1
180	59 ± 1	0.13 ± 0.01	859 ± 1
210	51 ± 1	0.11 ± 0.01	1146 ± 1
240	42 ± 1	0.10 ± 0.01	1663 ± 1
270	67 ± 1	0.13 ± 0.01	674 ± 1
300	39 ± 1	0.10 ± 0.01	2001 ± 1

This is further supported by the data contained in the Inorganic Crystal Structure Database (ICSD) [25, 26] on BFTO systems of similar constituent mass ratios [27]. The crystalline grains are larger in the sample activated for 60 min compared to the ones found in the sample activated for 30 min, after which a decrease in size occurs and the minimum for the activation time of 240 min is reached (Tab. I, Fig. 3).We could explain this by considering the initial agglomeration of the particles in the starting powders and then finer grinding as the milling time increases. The size of crystallites increases once more in the sample activated for 270

min, which suggests that the energy of mechanochemical activation was spent on the formation of larger crystallites, which are sensitive to a further increase of the milling time and reduce in the sample activated for 300 min (Fig. 3).

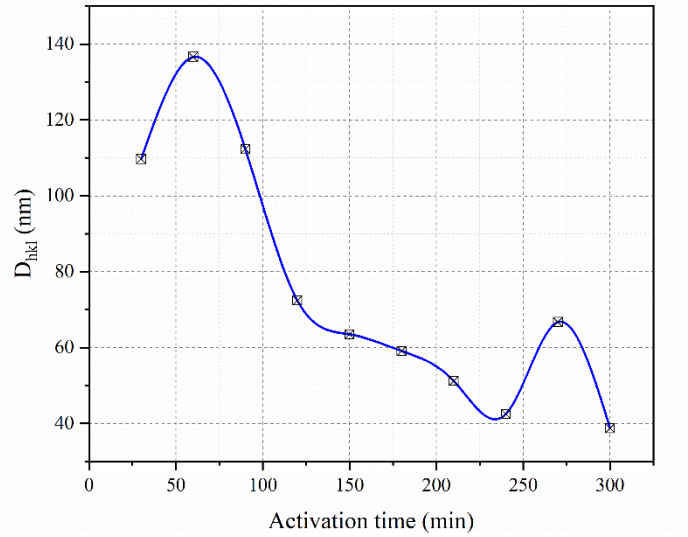

Fig. 3. Dependence of crystallites size of the Fe/$BaTiO_3$ system on the activation time.

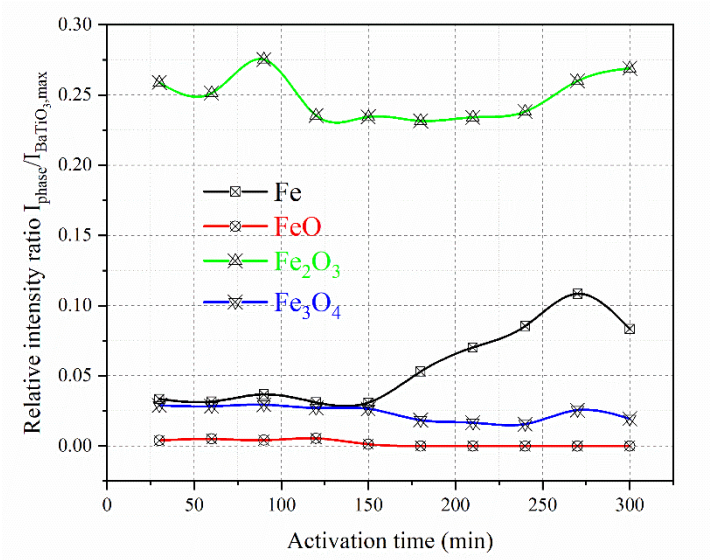

Fig. 4. Dependence of content of iron and its oxides on the activation time.

As the activation time increases, the system changes the content of iron and its oxides (Fig. 4). The content of Fe_2O_3 in the system shows a maximum for the activation time of 90 min.Further increase of the activation time leads to observed decrease in FeO and Fe_3O_4 content and a simultaneous increase in the content of iron from the activation time of 150 min onwards, with the BTO structure now progressing from cubic to hexagonal symmetry [28].The large increase in Fe content in comparison to the relatively small decrease in the content of wustite and magnetite phases could be attributed to the fact that a total of four iron atoms can be released from single molecules of FeO and Fe_3O_4, which give inasmuch intense XRD trace. In the sample activated for 270 min the Fe content reaches its highest value and this is followed by local maxima in both crystallite size and microstrain, as well as a minimum in dislocation density (Figs. 5 and 6), which may indicate the incorporation of iron

from FeOand Fe_3O_4 phases into the structure of barium titanate. By further increasing the time of milling (in the sample activated for 300 min), the iron begins to leave the BTO matrix, switching to hematite form.

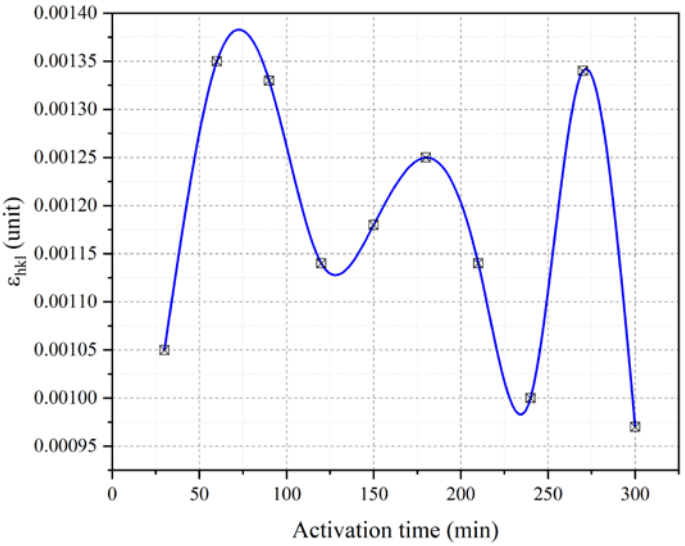

Fig. 5. Dependence of microstrain on the activation time.

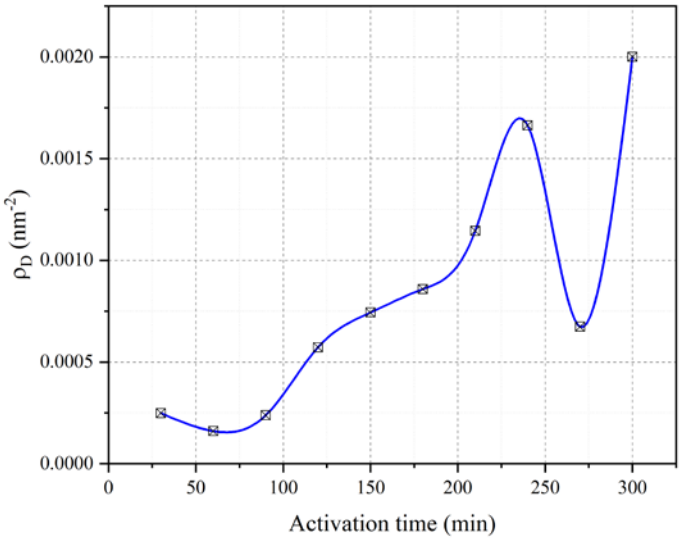

Fig. 6. Dislocation density as a function of the activation time.

Complex dielectric permittivity changes with the activation time (Fig. 7) showing a minimum value of 176.9 pF/m in the sample activated for 90 min, while reaching a maximum of 918.1 pF/m in the sample activated for 180 min.A local minimum of 548.2 pF/m (Fig.7) was observed for the sample activated for 150 min. The assumed migration of ferro and especially ferri ions into the BTO lattice leads to a structural phase transition and displacement of the ions inside the lattice, thereby changing the local dipole structure in the grains. The distribution of iron at grain boundaries affects the electrical properties of the system as well, reducing mobility of the walls between polarization domains [29, 30]. This is in agreement with the defective dipole model [31], according to which iron effectively immobilizes dipoles in its surroundings. Above the activation time of 180 min, increase in the content of

incorporated iron reduces the value of the dielectric constant to a final value of 304.6 pF/m in the sample activated for 300 min. Structural changes of the BFTO matrix also change the frequency response of the system (Fig. 8).

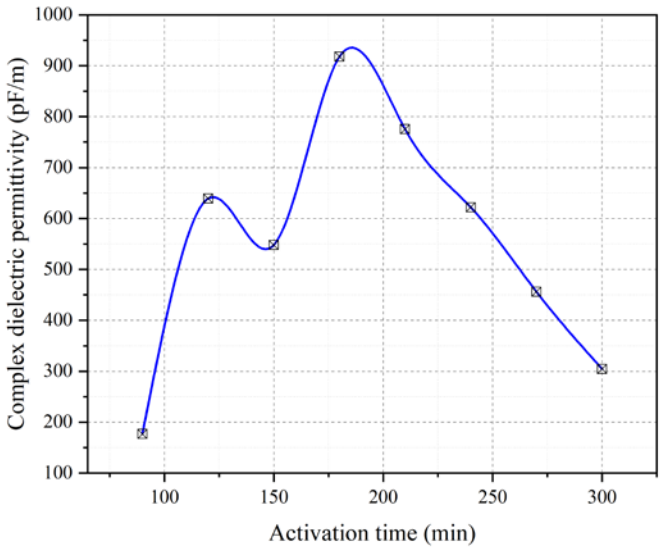

Fig. 7. Dependence of complex dielectric permittivity of the Fe/$BaTiO_3$ system on the activation time.

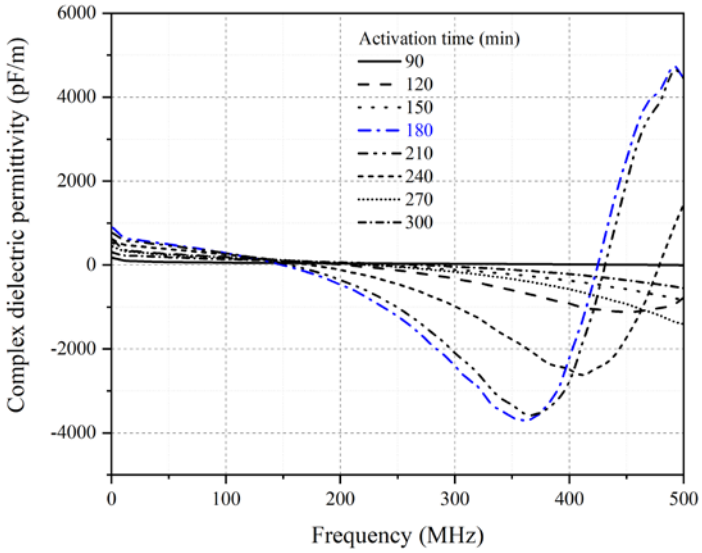

Fig. 8. Frequency dependence of a complex dielectric permittivity for different activation times.

The largest change is shown by the complex permittivity of the sample activated for 180 min, moving into the domain of negative values within the interval from 149.5 MHz to 425.0 MHz of the applied field. It is known that negative permittivity, which characterizes an entire class of synthetic materials called metamaterials [32], depends primarily on the structure of the system rather than the composition [33]. As the frequency of the external electric field increases, the dipole moments begin to progressively retard with their reorientation, which may lead to a decrease in permittivity. The inherent inertia of polarization contributes to the Brownian energy dissipation of the system-applied field interaction, with the dissipation

factor, as a measure of these processes, increasing (Fig. 9a). The permittivity of the sample activated for 180 min reaches a minimum in the 361.0 MHz frequency field and overall shows the dependence on the frequency of applied field typical for metamaterials.

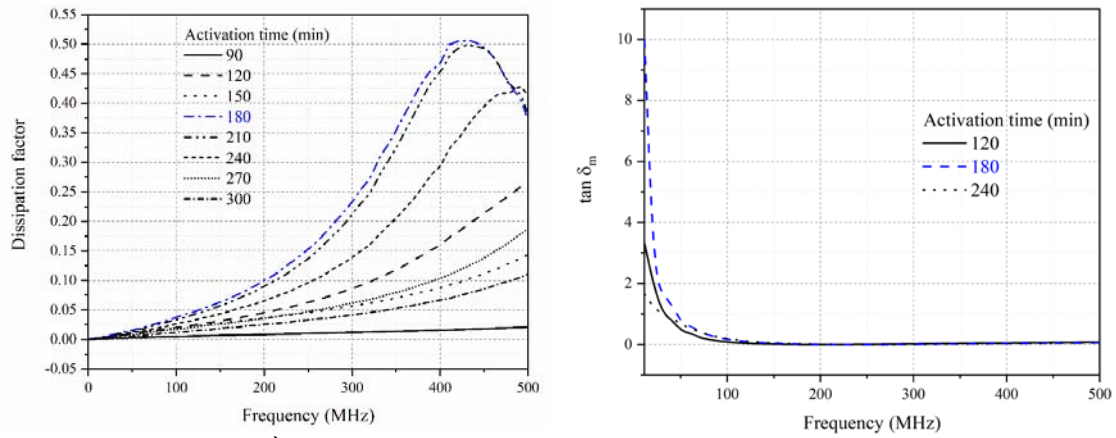

Fig. 9. a) Frequency dependence of the dissipation factor depending on the activation time. **b)** Magnetic losses in the given samples.

The evolution of complex magnetic permeability indicates that the system enters resonant excitation, i.e. ferromagnetic resonance (FMR) [34] in the applied oscillating field (Fig. 10). The shift of the FMR frequency to higher values with increase of the activation time is noticeable. This might mean that the mechanochemical activation of the system perturbs the damping constant of Larmor precession [35] of the electron intrinsic magnetic moments, due to the influence of arrangement within the magnetic domains of the samples. The losses of magnetic interactions fall exponentially close to zero value near the field frequency of about 200 MHz, while the dissipation factor of electrical interactions simultaneously begins to transition from linear to exponential growth (Fig. 9 a, b). The apparent complementarity of electrical and magnetic losses in the system makes it a good material for use in the controlled absorption of electromagnetic waves in the radio frequency domain.

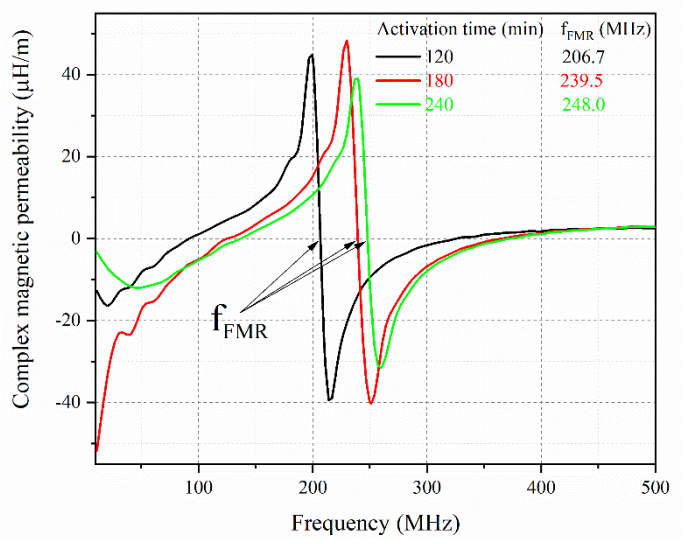

Fig. 10. Ferromagnetic resonance of the Fe/$BaTiO_3$ system exhibited in the radiofrequency field.

Fig. 11 exhibits the change of resistance in the full range of applied external field for samples activated for 120 min, 180 min and 240 min. The decrease in electrical resistance with rising frequency of the applied field follows a similar progression for all of the three samples. In accordance with Koops' phenomenological theory [36] crystallites, more conductive in their interior (mass), are separated by the weakly conducting boundaries of grains. Reducing the size of crystallites leads to an increase in contact, i.e. boundary surface between them. However, at the same time the amount of iron that migrates into the BTO matrix increases, therefore the experimental curves could be explained by the superposition of these influences. Negative values of resistance with the rise of frequency of the external field were attributed to the Hall effect [37] and dynamic distribution of charge carriers in the system.

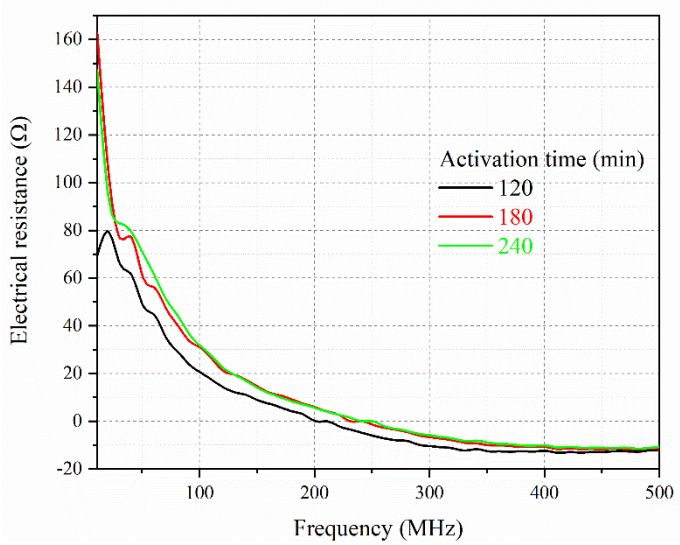

Fig. 11. Frequency dependence of electrical resistance for the samples milled for 120 min, 180 min and 240 min.

Tab. II Values of partial demagnetization temperature (t_d) and Curie temperature (t_C) of the given samples.

Heating cycle	Activation time (min)	t_d (°C)	t_C (°C)
I	90	212.4 ± 0.1	511.7 ± 0.1
	120	228.5 ± 0.1	560.7 ± 0.1
	240	238.8 ± 0.1	561.4 ± 0.1
	300	231.2 ± 0.1	538.6 ± 0.1
II	90	202.3 ± 0.1	497.6 ± 0.1
	120	226.5 ± 0.1	545.3 ± 0.1
	240	230.4 ± 0.1	556.1 ± 0.1
	300	226.1 ± 0.1	533.1 ± 0.1

The change in mass magnetization value during the successive heating and cooling cycles performed in a constant, weak magnetic field, in the range from 20 to 600 °C, for the selected samples, is given in Fig. 12. Magnetization of all of these samples shows a similar trend upon heating, decreasing slightly to ~225 °C, followed by a drop due to the phase transition caused by partial destruction of the domain structure within the crystallites. The external field slows down the further decrease of magnetization via the induction [38], up to ~538 °C when the thermal excitation completely prevails and the system switches from ferromagnetic to paramagnetic phase. Values of the partial demagnetization temperature (obtained from the -

(dM/dT) = f(T) peaks), as well as of the Curie temperature for both of the heating and cooling cycles are displayed in Tab. II.

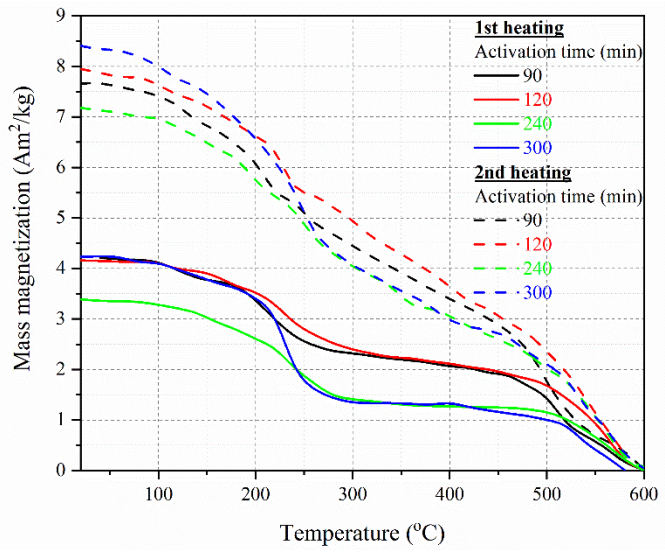

Fig. 12. Temperature dependence of mass magnetization of the samples milled for 90, 120, 240 and 300 min in the applied magnetic field of 50 kA/m.

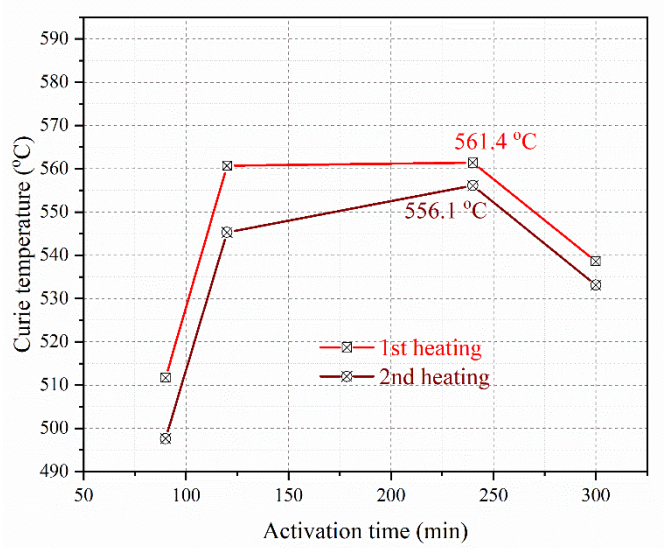

Fig. 13. Dependence of Curie temperature on the milling time.

Fig. 12 displays the thermal treatment leading to an increase of magnetization in all of the samples, caused by relaxation of the BFTO structure and simultaneously occurring processes of defects and microstrain annihilation [39]. After the first thermal cycle, magnetizations of all of the samples obtain higher values due to interaction of the system with the applied field during the cooling to room temperature. The most pronounced increase of about 95% shows a sample activated for 300 min. It is apparent that the activation time influences the magnetization of the system (Fig. 13) with the Curie temperature reaching the highest measured value in the sample activated for 240 min for both heating. In this sample crystalline grains are relatively the smallest (Fig. 3) and thus their total surface area is the largest compared to the ones in other samples. It is possible that the iron on the surface of

grains (which is now more abundant owing to the larger grain surface available), through the mechanisms of immobilization of neighboring dipoles, manages to amortize the thermal destruction of magnetic domains and move the Curie temperature to 561.4 °C. As shown in Fig. 13, the dependence of Curie temperature on the activation time manifests similar tendency during both the first and the second heating.

4. Conclusion

The study of multiferroics has been current for years, bearing in mind the scope and importance of possible applications in the technologies of the modern and increasingly demanding world. BFTO samples, with 30 mass% Fe and 70 mass% $BaTiO_3$, were mechanochemically activated for time duration ranging from 30 min to 300 min, sintered and then subjected to various methods of structural and functional characterization. With the increase of milling time, BTO changes its crystallinity, moving from orthorhombic and tetragonal to cubic symmetry. Change in size of the crystallites, microstrain value and dislocation density is a complex function of the activation time, with their changes being largely complementary. The highest content of Fe was found to be in the sample activated for 270 min and of Fe_2O_3 in the sample activated for 90 min. Migration of Fe^{3+} ions into the BTO lattice, as well as the distribution of iron at the grain boundaries, could explain the change of complex dielectric permittivity in the external field with frequencies up to 500 MHz. The highest permittivity of 918.1 pF/m was observed in the sample activated for 180 min. The system exhibits ferromagnetic resonance and a shift of the FMR frequency towards higher values with increase of the activation time is observed. A drop in magnetic losses near the frequency of the applied field of about 200 MHz is accompanied by an increase in electrical losses. Electrical resistance decreases with the rise of frequency of the field and has a similar progression for all of the analyzed samples. The evolution of mass magnetization with heating and cooling in an external magnetic field of 50 kA/m, shows a partial demagnetization of the system near the temperature of 225 °C and transformation from ferromagnetic to paramagnetic phase at a Curie temperature of approximately 538 °C. These critical values depend on the activation time and the highest Curie temperature of 561.4 °C was observed in the sample activated for 240 min. After heating and cooling in the applied field, the largest increase in mass magnetization was recorded in the sample activated for 300 min, amounting to about 95%.

Acknowledgments

This study was supported by the Ministry of Education, Science and Technological Development of the Republic of Serbia, Grants No. OI 172057.

5. References

1. M. M. Vopson, Fundamentals of Multiferroic Materials and Their Possible Applications,Crit. Rev. Solid State Mater. Sci. 40 (2015) 223-250,
2. P. Curie, Sur la symétrie dans les phénomènes physiques, symétrie d'un champ électrique et d'un champ magnétique (On symmetry in physical phenomena, symmetry of an electric field and a magnetic field), J. Phys. Theor. Appl. 3 (1894) 393-415.
3. J. F. Scott, Data storage: Multiferroic memories, Nat. Mater. 6 (2007) 256-257.

4. M. Bibes, A. Barthélémy, Multiferroics: Towards a magnetoelectric memory, Nat. Mater. 7 (2008) 425-426.
5. C. W. Nan, M. I. Bichurin, S. Dong, D. Viehland, G. Srinivasan, Multiferroic magnetoelectric composites: Historical perspective, status, and future directions, J. Appl. Phys. 103 (2008) 031101-031101.
6. Y. Tokura, Multiferroics as Quantum Electromagnets, Science 312 (2006) 1481-1482.
7. N. A. Spaldin, M. Fiebig, The Renaissance of Magnetoelectric Multiferroics, Science 309 (2005) 391-392.
8. I. E. Dzyaloshinskii, On the Magneto-Electrical Effect in Antiferromagnets, Sov. Phys. J. Exp. Theor. Phys. 10 (1960) 628-629.
9. C. Lacroix, P. Mendels, F. Mila, Introduction to Frustrated Magnetism: Materials, Experiments, Theory, Springer Series in Solid-State Sciences 164, Springer-Verlag Berlin Heidelberg, 2011.
10. C. Lu, M. Wu, L. Lin, J.-M. Liu, Single-phase multiferroics: new materials, phenomena and physics, Natl. Sci. Rev. 6 (2019) 653-668.
11. S. Rajan, P. M. M. Gazzali, L. Okrasa, G. Chandrasekaran, Multiferroic and magneto-dielectric properties in Fe doped $BaTiO_3$, J. Mater. Sci: Mater. Electron. 13 (2018) 11215-11228.
12. Z. B. Vosika, V. V. Mitić, G. M. Lazović, Lj. Kocić, Discrete Temperature Values in the Sintering Process as a $BaTiO_3$-ceramics Properties Parameter, Sci. Sinter. 49 (2017) 469-477.
13. V. Vučković, V. V. Mitić, Lj. Kocić, V. Nikolić, The Fractal Nature Approach in Ceramics Materials and Discrete Field Simulation, Sci. Sinter. 50 (2018) 371-385.
14. G. S. Upadhyaya, Sintering in Global Material Perspective, Sci. Sinter. 50 (2018) 501-508.
15. G. K. Williamson, W. H. Hall, X-ray Line Broadening from Filed Aluminium and Wolfram, Acta Metall. 1 (1953) 22-31.
16. P. Scherrer, Bestimmung der Größe und der inneren Struktur von Kolloidteilchen mittels Röntgenstrahlen (Determination of the size and internal structure of colloid particles using X-rays), Nachr. Ges. Wiss. Gött. Math.-Phys. Kl. (1918) 98-100, https://eudml.org/doc/59018.
17. G. K. Williamson, R. E. Smallman, III. Dislocation densities in some annealed and cold-worked metals from measurements on the X-ray Debye-Scherrer spectrum, Philos. Mag. 1 (1956) 34-46.
18. B. L. Morris, A. Wold, Faraday Balance for Measuring Magnetic Susceptibility, Rev. Sci. Instrum. 39 (1968) 1937.
19. R. T. Downs, M. Hall-Wallace, The American Mineralogist Crystal Structure Database, American Mineralogist 88 (2003) 247-250.
20. M. Quirós, S. Gražulis, S. Girdzijauskaitė, A. Merkys, A. Vaitkus, Using SMILES strings for the description of chemical connectivity in the Crystallography Open Database, Journal of Cheminformatics 10, 23 (2018), https://doi.org/10.1186/s13321-018-0279-6.
21. A. Jain, S. P. Ong, G. Hautier, W. Chen, W. D. Richards, S. Dacek et al, Commentary: The Materials Project: A materials genome approach to accelerating materials innovation, APL Mater. 1 (2013) 011002.
22. S. P. Ong, W. D. Richards, A. Jain, G. Hautier, M. Kocher, S. Cholia et al, Python Materials Genomics (pymatgen): A Robust, Open-Source Python Library for Materials Analysis, Comput. Mater. Sci. 68 (2013) 314-319.
23. K. Momma, F. Izumi, VESTA 3 for three-dimensional visualization of crystal, volumetric and morphology data, J. Appl. Crystallogr. 44 (2011) 1272-1276.

24. M. H. Frey, D. A. Payne, Grain-size effect on structure and phase transformations for barium titanate, Phys. Rev. B 54 (1996) 3158-3168.
25. G. Bergerhoff, I. D. Brown, Crystallographic Databases (International Union of Crystallography, Chester, UK, 1987).
26. D. Zagorac, H. Muller, S. Ruehl, J. Zagorac, S. Rehme, Recent developments in the Inorganic Crystal Structure Database: theoretical crystal structure data and related features, J. Appl. Crystallogr. 52:5 (2019), 918-925.
27. V. M. Nassif, R. E. Carbonio, J. L. Hodeau, E. Dooryhée, X-Ray Structural Determination of a Multilayered Magnetic Dielectric Ceramic $Ba_{42}Ti_{51}Fe_{20}O_{174}$ in the $BaO–TiO_2–Fe_2O_3$ System, J. Solid State Chem. 166 (2002) 400-414.
28. I. E. Grey, C. Li, L. M. D. Cranswick, R. S. Roth, T. A. Vanderah, Structure Analysis of the 6H–Ba(Ti, Fe^{3+}, Fe^{4+})$O_{3-\delta}$Solid Solution, J. Solid State Chem. 135 (1998) 312-321.
29. U. Knauer, Distribution of the iron dopant in barium titanate ceramic determined by the scanning transmission electron microscope, Phys. Status Solidi (a) 53 (1979) 207-210.
30. H. Heydrich, U. Knauer, Grain boundary effects in ferroelectric barium titanate, Ferroelectrics 31 (1981) 151-156.
31. J. Liu, L. Jin, Z. Jiang, L. Liu, L. Himanen, J. Wei et al, Understanding doped perovskite ferroelectrics with defective dipole model, J. Chem. Phys. 149 (2018) 244122.
32. E. Ozbay, K. Guven, K. Aydin, Metamaterials with negative permeability and negative refractive index: experiments and simulations, J. Opt. A: Pure Appl. Opt. 9 (2007) S301-S307.
33. B. Li, G. Sui, W.-H. Zhong, Single Negative Metamaterials in Unstructured Polymer Nanocomposites Toward Selectable and Controllable Negative Permittivity, Adv. Mater. 21 (2009) 4176-4180.
34. O. Yalçin, Ferromagnetic Resonance – Theory and Applications, InTech, Rijeka, 2013.
35. A. Baral, S. Vollmar, H. C. Schneider, Magnetization Dynamics and Damping due to Electron-Phonon Scattering in a Ferrimagnetic Exchange Model, Phys. Rev. B 90 (2014) 014427.
36. C. G. Koops, On the Dispersion of Resistivity and Dielectric Constant of Some Semiconductors at Audiofrequencies, Phys. Rev. 83 (1951) 121-124.
37. C. L. Chien, C. R. Westgate, The Hall Effect and Its Applications, Conference Proceedings edition, Plenum Press, New York, 1980.
38. J. Stöhr, H. C. Siegmann, Magnetism: From Fundamentals to Nanoscale Dynamics, Springer Series in Solid-State Physics, Springer, Berlin, 2006.
39. Z. Ristanović, A. Kalezić-Glišović, N. Mitrović, S. Đukić, D. Kosanović, A. Maričić, The Influence of Mechanochemical Activation and Thermal Treatment on Magnetic Properties of the $BaTiO_3$-Fe_xO_y Powder Mixture, Sci. Sinter. 47 (2015) 3-14.

Сажетак: *Мултифероични системи привлачни су истраживачима широм света услед разноликости како у постојећим, тако и у могућим новим применама. Да бисмо допринели разумевању процеса који се одвијају унутар структуре једног таквог система, подвргли смо га механохемијској активацији и топлотном третману. Смеше прахова гвожђа и баријум-титаната у масеном односу 30% Fe и 70% $BaTiO_3$ активиране су у планетарном млину у временском интервалу од 30 до 300 мин и потом синтероване на 1200 °C у атмосфери ваздуха. Током активирања систем трпи структурне фазне прелазе, при чему се мења садржај гвожђа и његових оксида. Највиши садржај Fe примећен је у узорку активираном 270 мин, уз локалне максимуме*

у величини кристалних зрна и вредности микронапрезања и минимум у густини дислокација. Комплексна диелектрична пропустљивост мења се у примењеном радиофреквентном пољу крећући се од 176,9 pF/m у узорку активираном 90 min до 918,1 pF/m у узорку активираном 180 мин. Како се фреквенција поља повећава, приметан је експоненцијални пад магнетних губитака енергије уз истовремен пораст електричних губитака енергије. Систем показује феромагнетну резонанцију, при чему дуже активирање у млину помера резонантну фреквенцију ка вишим вредностима. Негативни електрични отпор опажен је у свим анализираним узорцима. Време активирања мења температуру демагнетизације и Киријеву температуру узорака који пролазе кроз циклусе грејања и хлађења у спољашњем сталном магнетном пољу. Киријева температура је највиша у узорку активираном 240 мин. Топлотни третман повећава полазну магнетизацију у свим узорцима, са најизраженијим порастом од ~95 % у узорку активираном 300 мин.

***Кључне речи**:баријум-титанат, млевење, структура, електрична својства, магнетна својства.*